HST Photometry of trans-Neptunian Objects

D.C. Stephens (stephens@stsci.edu) and K.S. Noll
Space Telescope Science Institute

W.M. Grundy, R.L. Millis, J.R. Spencer and M.W. Buie
Lowell Observatory

S.C. Tegler
Northern Arizona University

W. Romanishin
University of Oklahoma

D.P. Cruikshank
NASA Ames Research Center

Abstract. ¿From July 2001 to June 2002, an *HST* snapshot program obtained *V*, *R* and *I* photometry for 72 TNOs. The TNOs were sorted by dynamical class, and Spearman rank correlation statistics were calculated for each combination of color and orbital parameter. No strong correlations were found for the combined sample of TNOs, the resonant TNOs, or the non-resonant TNOs (classical). The results presented here suggest that if correlations reported by other authors are real, they are evident only at shorter wavelengths than observed in our survey.

Keywords: trans-Neptunian objects, Colors, Correlations

1. Introduction

Photometric observations of trans-Neptunian Objects (TNOs) have consistently revealed a large range of colors from just blue of solar to extremely red (e.g. **?**, **?**; **?**, **?**). This diversity suggests variations in the surface composition of these bodies that may be attributable to their orbital evolution and past resurfacing history. If distinct correlations between colors and orbital parameters can be identified for TNOs as a function of dynamical class, the results may constrain the relative importance of resurfacing mechanisms suspected of contributing to the color distribution of TNOs.

Several possible correlations between the orbital parameters and colors of TNOs have been identified: a bi-modal color distribution in *B*-*V* vs. *V*-*R* (**?**, **?**, **?**, **?**), a correlation between *B*-*R* and inclination for the non-resonant (classical) TNOs (**?**), correlations between inclination, eccentricity, and color (most strongly in *B*-*R*) for the non-resonant TNOs (**?**), and correlations in *B*-*V*, *B*-*R*, and *B*-*I* with inclination, eccentricity, perihelion, and mean excitation velocity (v_{rms}) for the non-resonant

TNOs (?). So far, these results seem to suggest that the non-resonant TNOs are the only dynamical class for which significant correlations between color and orbital parameters exist.

2. Observations

During *HST* Cycle 10 (July 2001 – June 2002) we initiated a snapshot program to obtain multicolor photometry for a large number of TNOs using the Wide Field Planetary Camera 2 (WFPC2) on the Hubble Space Telescope (*HST*). An object list with 150 TNOs was submitted for observation, from which the *HST* scheduling team randomly selected targets throughout the year to fill holes in the observing calendar. This resulted in the observation of 72 (apparently) single TNOs, and 3 binary systems. The only selection criteria imposed for inclusion in the target list was that the orbital position of each TNO be known to better than 30 arcseconds, and have a predicted V magnitude between 22 to 24. Therefore, no intentional observational or classification bias was introduced into the resulting sample of TNOs observed with *HST*.

Two observing sequences were defined to optimize the science return. For targets with expected V magnitudes brighter than 23.5, two 160 second observations were acquired in each of the F555W ($\sim V$), F675W ($\sim R$), and F814W ($\sim I$) filters. Errors for these observations were typically at the 3-5% level. For fainter objects, two 260 second integrations were obtained in just the F555W ($\sim V$) and F814W ($\sim I$) filters. These observations have larger errors typically at the 7-8% level. In many cases, the observed V magnitude was fainter than predicted, and some objects with V magnitudes fainter than 23.5 were observed using all three filters with typical errors at the 6-7% level. Due to the significantly lower sensitivity of the WFPC2 instrument at shorter wavelengths, B-band photometry was not obtained for any of the TNOs.

Each observing sequence began with a single F555W exposure, followed by two exposures each in the F675W (where applicable) and F814W filters, and ended approximately 20 minutes later with another F555W exposure to monitor for rotation or light curve effects. During the 20 minutes that elapsed between the two F555W exposures, no variations in magnitude greater than the measurement precision of the observations were found for any of the TNOs. At the conclusion of the program, F555W ($\sim V$) and F814W ($\sim I$) magnitudes were successfully acquired for the 72 TNOs, of which 51 were also observed with F675W ($\sim R$).

The photometry acquired with *HST* benefited from the use of a well-understood instrument with a stable, compact PSF. Hence, data reduction for each TNO was identical and a number of documented corrections were applied to improve the photometry. First, each image was dark-subtracted using the most up-to-date files, flat-fielded, and pairs of images were combined to remove cosmic rays. Next, corrections for geometric distortion and the "34th row effect" were applied, and the flux within a 0.3" radius was determined. Model PSFs with parameters specific to each TNO were then generated using Tiny Tim software to correct the measured flux to an 0.5" aperture. The standard *HST* absolute calibration was then used to convert the fluxes to magnitudes. Finally a correction for the charge transfer efficiency(CTE) was employed (**?**) and the WFPC2 magnitudes were transformed to the standard Johnson V and Cousins R and I systems using the *synphot* package and an appropriately reddened solar spectrum. The final result was a uniform set of photometry free from systematic errors introduced by variable observing conditions, and large enough to provide a statistically significant sample of objects.

3. Results - No Strong Correlations

To search for correlations as a function of class, we assigned each TNO to one of four categories based on the classification given by the Minor Planet Center (**?**). Divided this way, our sample contains 38 non-resonant objects (classical), 21 resonant objects, 4 scattered disk objects (SDOs), and 9 that could not be assigned. The 51 objects with R magnitudes include 23 non-resonant objects, 19 resonant objects, 3 SDOs, and 6 that could not be classified. For each TNO the orbital elements were obtained from either the Minor Planet Center TNO or Centaur orbital element lists (**?**, **?**, **?**).

The Spearman rank method (**?**) was applied to all the data to investigate the relationships between color and orbital parameter that might exist for the sample as a whole and for each dynamical class. Tables I, II and III present the Spearman rank correlation statistics found for all of the TNOs, the resonant TNOs, and the non-resonant TNOs. The first column identifies the total number of objects used to calculate the statistic. This number is larger for correlations involving the V-I color since some of the TNOs were not observed in R. Columns 2 and 3 identify the two quantities being compared. The abbreviations stand for: i=inclination, v_{rms}=mean excitation velocity, a=semi-major axis, e=eccentricity, q=perihelion distance, and H_V=absolute V magnitude. The fourth column gives the Spearman rank correlation statistic r_{corr}, which indicates the likelihood that a correlation between the two quantities exists. The closer this value is to 1 or -1, the stronger the

Table I. Spearman Rank-Order Correlations - All TNOs

Number of Objects	Quantity 1	Quantity 2	r_{corr}	σ
51	*V-R*	*R-I*	0.24	1.7
72	*V-I*	i (deg)	-0.27	2.3
		v_{rms}	-0.22	1.9
		a	0.01	0.1
		e	-0.14	1.2
		q	0.17	1.4
		H_V	-0.04	0.3
51	*V-R*	i (deg)	-0.17	1.2
		v_{rms}	-0.22	1.6
		a	0.01	0.1
		e	-0.10	0.7
		q	0.17	1.2
		H_V	0.04	0.3
51	*R-I*	i (deg)	-0.15	1.2
		v_{rms}	-0.05	1.6
		a	-0.02	0.1
		e	-0.06	0.7
		q	0.03	1.2
		H_V	-0.14	1

correlation (or anti-correlation), while a value closer to 0 indicates no correlation. Finally, the last column identifies the significance of the correlation statistic and is derived from the confidence level (1-P), where P is the probability that a correlation statistic of equal or greater value could have been derived from a non-correlated sample. Applying gaussian statistics, a 99.7% confidence level corresponds to a 3σ significance, 95.4% to 2σ and 68.2% to 1σ.

These tables illustrate that for the *HST* data, no significant correlations exist between the *V-I*, *V-R*, *R-I* colors and orbital elements of the combined sample of TNOs, the resonant TNOs, and the non-resonant TNOs within the precision of the measurements. In Table I, a correlation statistic greater than 0.3 is not obtained for any combination of parameters. This agrees with previous claims that no correlations exist

Table II. Spearman Rank-Order Correlations - Resonant TNOs

Number of Objects	Quantity 1	Quantity 2	r_{corr}	σ
19	*V-R*	*R-I*	0.41	1.7
21	*V-I*	i (deg)	-0.11	0.5
		v_{rms}	-0.16	0.7
		a	-0.16	0.7
		e	-0.11	0.5
		q	-0.23	1
		H_V	0.25	1.1
19	*V-R*	i (deg)	0.14	0.6
		v_{rms}	-0.12	0.5
		a	-0.32	1.3
		e	-0.29	1.2
		q	-0.01	0.1
		H_V	0.26	1.1
19	*R-I*	i (deg)	-0.29	1.2
		v_{rms}	-0.28	1.1
		a	-0.28	1.2
		e	-0.17	0.7
		q	-0.20	0.8
		H_V	0.21	0.8

when TNOs from different dynamical classes are combined (**?**, **?**; **?**, **?**). The correlation statistics for the resonant TNOs are presented in Table II. In this case, the largest correlation occurs between the *V-R* and *R-I* colors ($r_{corr} = 0.41$), but it is not significant at only 1.7σ. Finally Table III presents the correlation statistics for the non-resonant TNOs. As in Tables I and II, no strong correlations are found. Possible weak correlations are identified for the *V-R* color with inclination ($r_{corr} = -0.40$) and v_{rms} ($r_{corr} = -0.39$) but both results have a statistical significance of less than 2 σ.

It is possible that correlations exist but were not identified in our data set due to measurement accuracy and precision, and one can speculate that with higher accuracy and precision, a significant correlation might have been found. Typical *HST* photometry errors (5–7% in *V*

Table III. Spearman Rank-Order Correlations
- Non-resonant TNOs (Classical)

Number of Objects	Quantity 1	Quantity 2	r_{corr}	σ
23	*V-R*	*R-I*	-0.24	1.1
38	*V-I*	i (deg)	-0.25	1.5
		v_{rms}	-0.06	0.3
		a	0.04	0.2
		e	0.21	1.3
		q	-0.17	1.0
		H_V	0.02	0.1
23	*V-R*	i (deg)	-0.40	1.9
		v_{rms}	-0.39	1.8
		a	-0.29	1.4
		e	-0.24	1.1
		q	0.11	0.5
		H_V	0.11	0.5
23	*R-I*	i (deg)	-0.10	0.5
		v_{rms}	0.10	0.5
		a	0.10	0.5
		e	0.30	1.4
		q	-0.29	1.3
		H_V	-0.17	0.8

and 5% in *R* and *I*) are similar to the 5% precision obtained by **?** (**?**) and **?** (**?**), and both of these data sets found significant correlations (3-4 σ) between the *B*-band colors and inclination for the non-resonant TNOs. Therefore, we would expect that with a uniform sample of 23 and 38 non-resonant TNOs, if any correlations similar in size exist for the *HST* data, they would have been identified.

Within the accuracy of the *HST* photometry, no Spearman rank correlations were found for any combination of *V-I*, *V-R*, or *R-I* color with orbital characteristic. Therefore, either previous claims of Spearman rank correlations between color with inclination angle, v_{rms}, eccentricity, and perihelion distance reported for the non-resonant TNOs are spurious, or are only valid for colors that include the *B* magnitude. If the latter is true, it suggests that either the mechanism most responsible

Table IV. Spearman Rank-Order Correlations for Non-resonant TNOs From Other Studies

Number of Objects	Quantity 1	Quantity 2	r_{corr}	σ	reference
17	*V-I*	i (deg)	-0.28	1.1	?, ?
21	*V-R*		-0.44	2.0	?, ?
17	*R-I*		-0.21	0.8	?, ?
25	*V-R*		-0.57	3.0	?, ?, ?, ?
13	*V-R*		-0.34	1.1	?, ?
32	*V-I*		-0.39	2.2	?, ?
52	*V-R*		-0.40	3.0	?, ?
32	*R-I*		-0.32	1.8	?, ?

for the correlation is only active at shorter wavelengths, or is masked at longer wavelengths by compositional diversity and/or other resurfacing effects.

4. Comparison with other *V*,*R*,*I* Results

The lack of a correlation between the *V*, *R*, *I* colors and orbital elements of the non-resonant TNOs is not unique to the *HST* data set. *V*, *R* and *I* magnitudes were also obtained for a large number of non-resonant TNOs by **?** (?), **?** (?, ?, ?) and **?** (?). From each of these papers the *V*, *R* and (where available) *I* magnitudes were extracted for each non-resonant TNO (as defined by the Minor Planet Center) and used to determine a Spearman rank correlation statistic for each color with orbital element. The statistics found for color and inclination angle are listed in Table IV, where the three **?** papers have been combined to create a larger sample of objects. Correlations found using data from **?** (?) were also included for completeness, though we note that their sample is a nonuniform compilation of photometry obtained from several different sources, including these papers.

The results in Table IV are essentially independent of one another and the *HST* values in Table III since only 20-40% of the non-resonant TNOs in one survey were also observed in a second survey. These numbers support the conclusion that no strong Spearman rank correlation for the *V*, *R* and *I* colors with inclination exists within a photometric accuracy of 5%. The only significant result is the 3σ correlation statistic between *V-R* and inclination ($r_{corr} = -0.57$) observed by **?** (?, ?, ?).

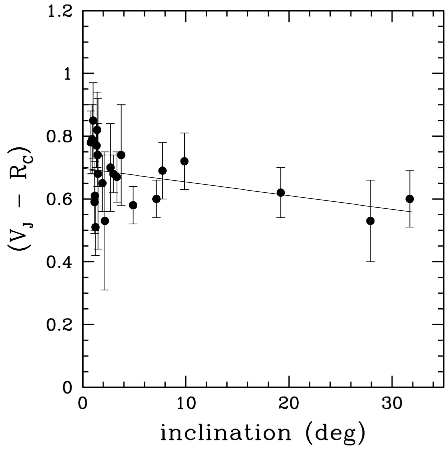

a. Inclination vs. (V-R)

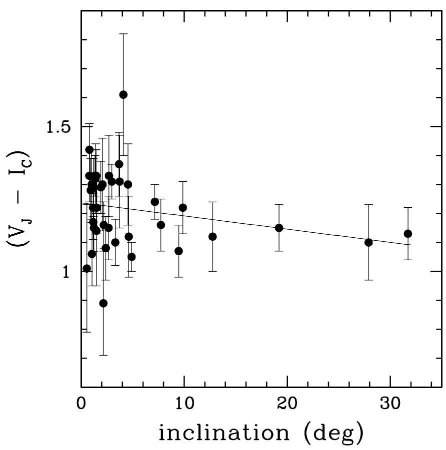

b. Inclination vs. (V-I)

Figure 1. Inclination vs. *HST* color for the non-resonant (classical) TNOs. A weighted linear least squares fit is plotted over the data.

This suggests that there may be a weak correlation in *V-R* with inclination, but we may not see this correlation since the HST magnitudes have larger uncertainties than those cited by **?** ($\sim$ 1-2%). Table IV indicates that correlations between inclination and the *V-I* and *R-I* colors are less likely to occur than a correlation between inclination and *V-R*. This may be consistent with the hypothesis that strong correlations with inclination are present only at shorter wavelengths.

5. Mixed Populations?

To get a visual intuition for what the Spearman rank correlation reveals about the *HST* data, we plotted the two strongest (non-significant) correlations with *V-R* and *V-I* for the non-resonant objects along with weighted linear least squares fits in Figure 1 (*V-R*, $r_{corr} = -0.40$, σ=1.9; *V-I*, $r_{corr} = -0.25$, σ=1.5). The linear least squares fits have negative slopes, but the uncertainties and scatter in the data allow for a range of slopes including the case of no trend in color as a function of inclination, in agreement with the low statistical significance found by the Spearman rank test for these parameters.

The main difference between our results and previous work that has found a correlation between color and inclination (**?**, **?**; **?**, **?**) is the larger number of objects in our data set and the fact that we find almost equal numbers of red and gray TNOs at low inclination. It remains possible to speculate that statistical tests failed to find correlations because of the presence of more than one population of TNO with different color and/or orbital properties in our samples (?) and our inability to separate out the distinct populations before applying the test. It may be that the current scheme for classifying TNOs is inadequate. If so, when new schemes for classifying TNOs are developed, our large and uniform data set provides an ideal resource for any future correlation searches.

6. Conclusions

We have obtained photometric measurements of 72 TNOs at optical wavelengths with WFPC2. This represents one of the largest and most uniform sets of optical photometry of TNOs available. We have searched for correlations of color with dynamical properties in the full data set and in two subsets, objects classified as non-resonant or "classical" TNOs and objects in any of the several resonances with Neptune. We find no statistically significant correlation with any combination of parameters.

Other authors have identified possible correlations using similar statistical tests. There are several possible explanations for this difference that we have considered. Because of the short integration times in the HST data, our errors are typically at the 5% level. Some other observers report errors as low as 1-2%. It is possible that weak correlations would be missed in our data set and found in others because of this difference. Another possible explanation we have noted is that significant correlations found by other workers have all utilized colors that include the B band magnitude. If these correlations are real, it suggests that the spectrally active component correlated with dynamical class may be in the blue portion of the spectrum.

Progress in identifying the source of color variations in TNOs will require additional multi-wavelength observations, a re-evaluation of TNO classification, and an accurate determination of the albedo. The significance of the *HST* results presented here will be enhanced in the future by PSF-fitting to reduce the uncertainties in optical photometry, the inclusion of near-infrared J and H magnitudes measured with NICMOS, and albedo measurements from SIRTF. The infrared data's sensitivity to solid state features will help identify objects with different surface compositions, and albedo measurements will ascertain whether these objects are gray due to resurfacing or extensive irradiation. The complexity and diversity of the Kuiper Belt ensures that this field will remain active for the foreseeable future.

References

Dolphin, A.: 2002, 'Netscape: WFPC2 Calibration and CTE Correction Updates (September 2002)', $http://www.noao.edu/staff/dolphin/wfpc2\_calib/$

Doressoundiram, A., et al.: 2002, 'The Color Distribution in the Edgeworth-Kuiper Belt', *AJ* **Vol. 124**, pp. 2279-2296

Hainaut, O.R., and Delsanti, A.C.: 2002, 'Colors of Minor Bodies in the Outer Solar System. A statistical analysis', *A&A* **Vol. 389**, pp. 641-664

Jewitt, D., and Luu, J.: 1998 'Optical-Infrared Spectral Diversity in the Kuiper Belt', *AJ* **Vol. 115**, pp. 1667-1670

Levison, H.F., and Stern, S.A.: 2001, 'On the Size Dependence of the Inclination Distribution of the Main Kuiper Belt', *AJ* **Vol. 121**, pp. 1730-1735

Marsden, B.G.: 2003a, 'Minor Planet Electronic Circular', $http://cfa-www.harvard.edu/iau/mpec/K03/K03J07.html$

Marsden, B.G.: 2003b, 'List Of Transneptunian Objects', $http://cfa-www.harvard.edu/iau/lists/TNOs.html$

Marsden, B.G.: 2003c, 'List Of Centaurs and Scattered-Disk Objects', $http://cfa-www.harvard.edu/iau/lists/Centaurs.html$

Press, W.H et al.: *Numerical Recipes in Fortran.* 2nd ed.; Cambridge University Press, Cambridge, 1992.

Tegler, S.C., and Romanishin, W.: 1998, 'Two distinct populations of Kuiper-belt objects', *Nature* **Vol. 392**, pp. 49-50

Tegler, S.C., and Romanishin, W.: 2000, 'Extremely red Kuiper-belt objects in near-circular orbits beyond 40 AU', *Nature* **Vol. 407**, pp. 979-981

Tegler, S.C., and Romanishin, W.: 2003, 'Resolution of the Kuiper belt object color controversy: two distinct color populations', *Icarus* **Vol. 161**, pp. 181-191

Trujillo, C.A., and Brown, M.E.: 2002, 'A Correlation between Inclination and Color in the Classical Kuiper Belt', *ApJL* **Vol. 566**, pp. L125-L128